Single-Loop All-Pass-Filter-based Active Damping for VSCs with LCL filters Connected to the Grid

Javier Roldán-Pérez*, Emilio Bueno†, R. Peña-Alzola‡, and Alberto Rodríguez-Cabero*
*IMDEA Energy Institute, Madrid, Spain.
†Alcalá de Henares University, Madrid, Spain.
‡University of Strathclyde, Glasgow, UK.

***Abstract*—LCL filters are commonly used to connect Voltage Sourced Converters (VSCs) to the grid. This type of filters are cheaper than a single inductor, but they can generate resonance problems if no active or passive damping method is used. Active damping methods are becoming popular in the literature because they improve efficiency, but they are sometimes difficult to implement and additional measurements are required. This paper proposes a method to provide active damping for VSCs connected to the grid that is based on making zero the open-loop phase at the resonance frequency. It will shown that this strategy provides adequate damping of oscillations and that it can be achieved in two different ways: at the design stage (if the design constraints make it possible) or with an all-pass filter in series with the current controller. All the proposed control algorithms are verified by simulation and in a 15 kW prototype of a three-phase VSC connected to the grid with an LCL filter.**

I. Introduction

LCL filters are popular in power electronics applications since they are commonly cheaper than a filter based on a single inductor. However, these filters generate a resonance that, in many cases, interacts the VSC current controller. Therefore, this resonance need to be damped either with additional passive elements or with a more sophisticated control system. The most common solution to damp the resonance is to add a resistor in series with the filtering capacitor of the *LCL* filter, what is commonly known as "passive damping" [1]. Passive damping reduces the converter efficiency and slightly deteriorates the high-frequency filtering capabilities of the *LCL* filter [2]. However, it is a simple solution so it is widely adopted when losses are not important. There are methods to reduce the damping resistor losses, but more hardware elements are required [3]. However, when passive damping cannot be applied, an adequate damping can be achieved with the control system: this is commonly known as "active damping" [4]. Active damping prevents the use of resistors, but additional state variables are sometimes required [5].

Multi-variable controllers can be used to damp the resonance of *LCL* filters [6, 7]. Between these controllers, the "virtual resistor" is commonly applied to emulate the behaviour of a resistance by using an inner control loop [8]. However, calculus and measurements delays reduce the validity of this method and a carefully-designed digital filter has to be added to the control loop [4, 8]. Moreover, additional sensors are sometimes required to measure the capacitor voltage [4] or current [9]. The resonance can also be damped with a state-feedback controller in order to place the closed-loop poles in appropriate locations [7]. State-feedback controllers are straightforward to design, but it is difficult to figure out which pole position leads to acceptable stability margins and, also, additional measurements are required [7, 10]. Alternatively, Huerta *et al.* [11] select the controller gains by using a linear-quadratic regulator. This solution simplifies the pole location problem, but the value of the weighting coefficients for the LQ problem may be difficult to find. Some authors use other multi-variable controllers to tackle resonance problems [6, 12]. However, multi-variable controllers require additional measurements compared to a control system based on a single loop. The latter problem can be solved with an observer [13], but this adds even more complexity to the control system. Additionally, Busada *et al.* [5] propose a high-order controller that makes possible to choose the closed-loop poles locations with a single loop, but the compensator obtained is complex so implementation problems may be difficult to solve.

For these reasons, single-loop control strategies are generally preferred and, among them, notch filters are a popular alternative [14]. This type of controllers are easy to design and implement, but they are sensitive to changes in the resonance frequency. Other types of solutions like artificial neural networks are sometimes used to damp the *LCL* filter resonance, but they are not very popular since their performance is difficult to predict and they are not easy to implement [15]. Hysteresis controllers can be used as well for active damping applications [16]. However, this control method is not straightforward to apply for high-order plants, which is the case of the *LCL* filter. Recently, the effects of delays in the open-loop transfer function of *LCL* filters have been studied by Lyu *et al.* [17], revealing that these effects can be used to damp *LCL* filter resonance. In this sense, Wang *et al.* [18] explore the effects of these delays taking into account the discrete-time implementation. A similar approach is followed by Chen *et al.* [19]. The results of these works are promising since they provide a simple solution to damp the resonance with a single control loop.

This paper proposes a method to provide active damping for VSCs connected to the grid with *LCL* filters. First of all, it will be shown that active damping can be provided at the design stage if the design constraints allow it. However, when this is not possible, an all-pass filter in series with the current controller is used with this purpose. With this addition,

a classical PI controller can be easily designed to control the grid-side current of the filter. It will be shown that this strategy provides large stability margins if a first-order all-pass filter is applied. The control techniques proposed in this paper are verified in a 15 kVA prototype of a VSC with an *LCL* filter.

II. Active Damping Overview

A. Description of the Control System

Fig. 1 shows the electrical diagram and the control system of a VSC connected to the grid with an *LCL* filter. A Synchronous Reference Frame (SRF) (dq) is used to simplify the controller implementation with a Phase Looked Loop (PLL) synchronized with the d-axis positive-sequence of the grid voltage [20]. Therefore, the instantaneous active power $(p(t))$ is controlled with $i_d(t)$, while the instantaneous reactive power $(q(t))$ is controlled with $i_q(t)$ [20]. The DC-link voltage is maintained constant with a diode rectifier directly connected to the grid.

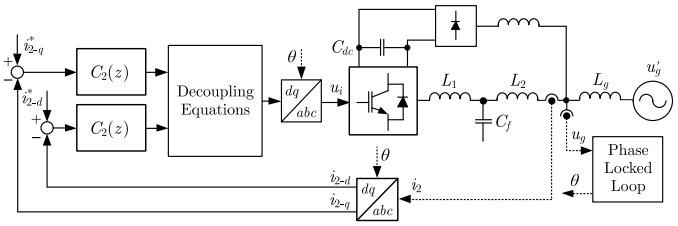

Fig. 1. Electrical diagram of a VSC with an *LCL* filter. The controlled variable is $i_2(t)$ and the diode rectifier maintains the DC-link voltage constant.

B. Modelling Equations

Assuming perfect decoupling between axis, the transfer function that relates $U_i(s)$ with $I_2(s)$ (Laplace transforms of $u_i(t)$ and $i_2(t)$, respectively) is

$$P(s) = \frac{b_1 s + 1}{a_3 s^3 + a_2 s^2 + a_1 s + a_0}, \tag{1}$$

where

$$\begin{aligned} a_0 &= R_1 + R_2, \\ a_1 &= L_1 + L_2 + C_f(R_d R_2' + R_d R_1 + R_1 R_2'), \\ a_2 &= C_f(L_2'(R_d + R_1) + L_1(R_d + R_2')), \\ a_3 &= C_f L_1 L_2', \\ b_1 &= C_f(R_d + R_2'), \end{aligned} \tag{2}$$

with $L_2' = L_2 + L_g$ and $R_2' = R_2 + R_g$. This transfer function typically contains a low-frequency pole, a pair of high-frequency complex poles, and a high-frequency zero. The complex-poles resonance frequency is [1]:

$$\omega_r = \sqrt{\frac{1}{C_f}\frac{L_2' + L_1}{L_2' L_1}}. \tag{3}$$

The plant in (1) can be discretized with the ZOH method, together with a number of delays due to computations and measurements (n), yielding [21]:

$$P_2(z) = z^{-n} Z\left\{P(s)\right\}_{ZOH}. \tag{4}$$

C. Classical Current Controller with LCL Filters

A PI controller can be used to track constant set-points of i_{2-d} and i_{2-q} if the grid voltage is balanced. Therefore:

$$C_2(z) = K_p + K_i z/(z-1). \tag{5}$$

Fig. 2 shows $P_2(e^{j\omega t_s})$ and $G_2(z) = P_2(z)C_2(z)$, where $C_2(z)$ is a PI controller designed with a phase margin (ϕ_m) of 65 degrees. The system parameters are defined in Section VI-A. It can be seen that the phase of $G_2(e^{j\omega t_s})$ is hardly modified at high frequency. Therefore, it is clear that the damping problem cannot be solved with this type of controller.

D. Proposed Active Damping Solution

The core of the active damping method proposed in this paper is to guarantee zero phase at the resonance frequency:

$$G_2(e^{j\omega_r t_s}) = A_g e^{j\phi_g}, \ \text{ with } \ \phi_g = 0 \text{ deg}. \tag{6}$$

This condition guarantees that the open-loop frequency response at the resonance frequency is purely resistive. It will shown that this choice a) provides adequate resonance damping and b) maximizes the phase margins. Two alternatives to achieve $\phi_g = 0$ will be explored:

1) Active Damping at the Design Stage: With this method a) the resonance frequency (ω_r) or b) the sampling period (t_s) are modified so that $\phi_g = 0$ deg without any addition to the control system.

2) Active Damping with All-Pass Filters: If active damping cannot be provided at the design stage due to design constraints (e.g. ω_r and t_s are fixed), a unitary-gain all-pass filter [22], called $D(z)$, is proposed (see Fig. 3):

$$G_2(z) = C_2(z)D(z)P_2(z), \tag{7}$$

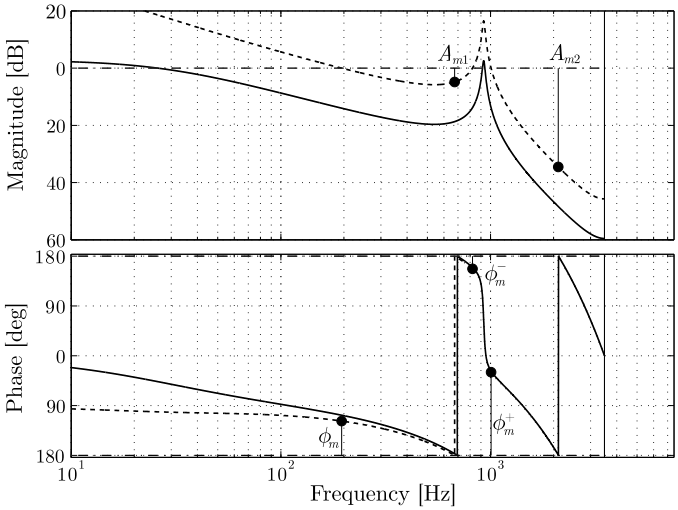

Fig. 2. Frequency response of (solid) $P_2(z)$ and (dotted) $G_2(z)$, where $C_2(z)$ is PI controller with $\phi_m = 65$ deg (no active damping is used). $f_s = 7$ kHz.

where

$$G_2(e^{j\omega_r t_s}) = \underbrace{(A_c e^{j\phi_c})}_{C_2(e^{j\omega_r t_s})} \cdot \underbrace{(e^{j\phi_d})}_{D(e^{j\omega_r t_s})} \cdot \underbrace{(A_p e^{j\phi_p})}_{P_2(e^{j\omega_r t_s})} \quad (8)$$

and $|D(e^{j\omega t_s})| = 1\ \forall\omega$. To achieve $\phi_g = 0$ deg, the following condition must be fulfilled:

$$\phi_g = \phi_c + \phi_d + \phi_p = 0. \quad (9)$$

Therefore, ϕ_d can be chosen to ensure that (9) is satisfied. As $D(z)$ is an all-pass filter, only the phase is modified and high-frequency noise will not be amplified.

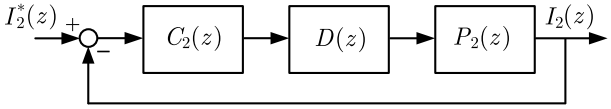

Fig. 3. Simplified control diagram of the controlled plant with $D(z)$.

III. Providing Active Damping at the Design Stage

As shown before, at high frequencies $\phi_c \approx 0$, so $\phi_g \approx \phi_p$. The value of ϕ_p can be estimated by analysing $P_2(z)$ (see Fig. 2 (solid)). First of all, the low-frequency pole contribution to ϕ_g is almost -90 deg. Secondly, the resonant poles provide almost no phase until their resonance frequency is reached, when the phase suddenly suffers a -180 deg phase shift at ω_r. Finally, the phase introduced by the delays is $-n\omega_r t_s$ rad, while the high-frequency zero has no phase contribution if $R_d = 0\ \Omega$. Taking into account all the considerations above, the condition that makes $\phi_g = 0$ deg is, approximately:

$$\exists k \in \mathbb{N}\ :\ \phi_p \approx -n\omega_r t_s - \pi = 2k\pi. \quad (10)$$

It is easy to see that there are only two alternatives to fulfil (10), which are to modify a) ω_r or b) t_s. However, design constraints can limit the applicability of this strategy. Clearly, the simplified formula in (10) can be replaced by the actual value of ϕ_p calculated with $P_2(e^{j\omega_r t_s})$, but (10) provides valuable information to understand the damping problem.

IV. Active Damping based on All-Pass Filters

An alternative for $D(z)$ is a first-order digital all-pass filter [22, 23]:

$$D'(z) = \frac{(1+d')z^{-1} + (1-d')}{(1-d')z^{-1} + (1+d')}, \quad (11)$$

where $d' \in (0,1)$ adjusts the phase of the filter at the resonance frequency. If $d' \notin (0,1)$, the filter is unstable. The phase of $D'(e^{j\omega t_s})$ at ω_r is [23]:

$$\phi'_d = 2\arctan\left(\frac{(1-d')\sin(\omega_r t_s)}{(1+d') + (1-d')\cos(\omega_r t_s)}\right) - \omega_r t_s. \quad (12)$$

Fig. 4 shows the phase of $D'(e^{j\omega t_s})$ for $f_s = 10$ kHz and $d' \in (0,1)$, while $|D'(e^{j\omega t_s})|$ is always one. The phase for a given value of ω_r (f_r in Hertz) can be modified with d', and the value that provides the required phase (ϕ'_d) can be solved from (12), yielding:

$$d' = \tan(\phi'_d/2)/\tan(\omega_r t_s/2). \quad (13)$$

As shown in Fig. 4, $D'(z)$ cannot provide any phase value between 0 and 360 deg. Therefore, if more phase is required, a higher-order all-pass filter can be used instead [23]. A simple solution is to include m filters like $D'(z)$ in series, yielding

$$D(z) = (D'(z))^m. \quad (14)$$

Now, ϕ_d can be divided between m filters and the phase of each one can be selected as:

$$\phi'_d = \phi_d/m. \quad (15)$$

The minimum and maximum phase that each filter can provide can be solved from (13) by making $d' = 0$ and $d' = 1$:

$$0 < \phi'_d < \omega_r t_s. \quad (16)$$

In order to calculate the number of $D'(z)$ filters required to provide ϕ_d, (15) and (16) can be merged, yielding:

$$m \geq \phi_d/(\omega_r t_s) \in \mathbb{N}. \quad (17)$$

The main drawback of this method is that the additional phase introduced by $D(z)$ can slow down the transient response.

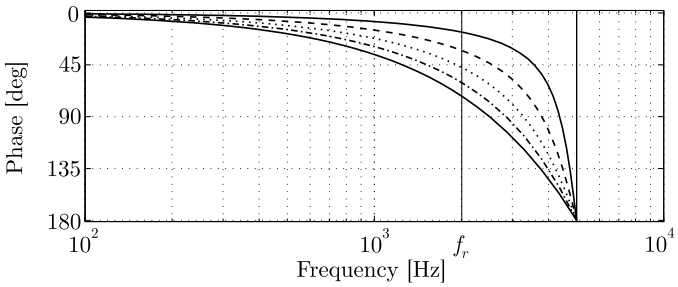

Fig. 4. Phase of $D'(e^{j\omega t_s})$, varying the value d'. From top to bottom, $d' = 0.1$, 0.3, 0.5, 0.7, and 0.9, for $f_s = 10$ kHz.

V. Practical Guide to Provide Damping

The concepts explained in Section III and IV to provide active damping can be applied as follows:

1) If possible, design the converter so that $\phi_p = 0$ deg (or $\phi_g = 0$). If this condition is met, $D(z)$ is not necessary and a PI controller can be used.

If ϕ_p differs to a great extend from zero, an all-pass filter can be used to provide active damping:

1) First, use (17) to calculate the number of $D'(z)$ filters (m) required to guarantee that $\phi_d = -\phi_p$.
2) Use (13) to calculate the value of d'.
3) Design $C_2(z)$ with a classical method, but taking into account that $D(z)$ is in series with $P_2(z)$.

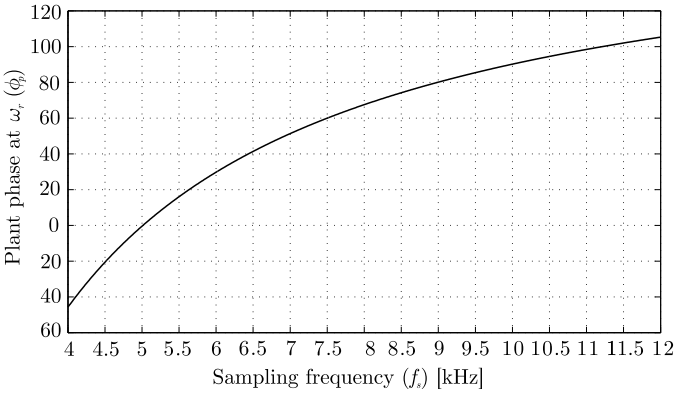

Fig. 5. Plant phase at the resonance frequency (ϕ_p) changing the sampling frequency (f_s) ($\phi_p = 0$ deg is obtained when $f_s = 5$ kHz).

VI. Case Study

A. System Description

The VSC parameters are $L_1 = 2.3$ mH ($R_1 = 70$ mΩ), $L_2 = 0.93$ mH ($R_2 = 30$ mΩ), and $C_f = 23.8$ μF ($R_d = 0$ mΩ). A transformer ($L_g = 1$ mH) is used to connect the VSC to grid. Therefore, $f_r = 1.27$ kHz without the transformer, and $f_r = 1.0$ kHz with it. Decoupling equations are used to control the dq-axis dynamics, independently [24]. The control system gives $n = 2$. The sampling (f_s) and switching (f_{sw}) frequencies are equal. Two designs has been carried out in order to highlight the contributions of this paper:

1) In the first case damping is achieved at the design stage
2) In the second case damping is provided with a first-order all-pass filter.

B. Achieving Damping at the Design Stage

Since the *LCL* filter values and n have been already set, only t_s can be modified to provide active damping at the design stage. Fig. 5 shows ϕ_p when f_s changes. For $f_s \approx 5$ kHz, $\phi_p \approx 0$ deg. Fig. 6 shows the frequency response of $P_2(z)$ and $G_2(z)$ when $f_s = 5$ kHz. The controller $C_2(z)$ has been calculated with $\phi_m = 45$ deg and implemented as shown in (5). The phase of $C_2(z)$ at ω_r is $\phi_c = -1$ deg, so it hardly affects ϕ_m^+ and ϕ_m^-. The phase margins are $\phi_m = 45$ deg, $\phi_m^- = -78.4$ deg, and $\phi_m^+ = 77.1$ deg, while $A_{m1} = 7$ dB and $A_{m2} = 22$ dB.

The oscillating frequency (ω_u) of the plant is 500 Hz, approximately, and it is slightly affected when $C_2(z)$ is applied.

C. Active Damping with First-Order All-Pass Filters

Fig. 7 shows the frequency response of $P_2(z)$ and $G_2(z)$ when $f_s = 9$ kHz and $D(z)$ compensates the plant phase at the resonance frequency (ϕ_p). The value of ϕ_p is 80.95 deg, so $D(z)$ is necessary. The minimum number of $D'(z)$ filters is calculated with (17), yielding $m = 2.002$. In this particular case, the equivalent phase required can be obtained by making $D(z) = z^{-2}$ since $m \approx 2$. However, to demonstrate the validity of the proposed design procedure, condition (17) is applied strictly so $m = 3$. Therefore, $D(z)$ is designed to provide $\phi_d = -\phi_p$, giving $d' = 0.65$. The controller $C_2(z)$ is calculated in continuous time with $\phi_m = 45$ deg. The phase margins are $\phi_m = 45$ deg, $\phi_m^- = -77.5$ deg, and $\phi_m^+ = 76.3$ deg, while the gain margins are $A_{m1} = 7.2$ dB, $A_{m2} = 21$ dB, and $A_{m3} = 44$ dB.

The plant oscillating frequency (ω_u) is approximately 850 Hz, and is reduced to 500 Hz when $D(z)$ and $C_2(z)$ are applied.

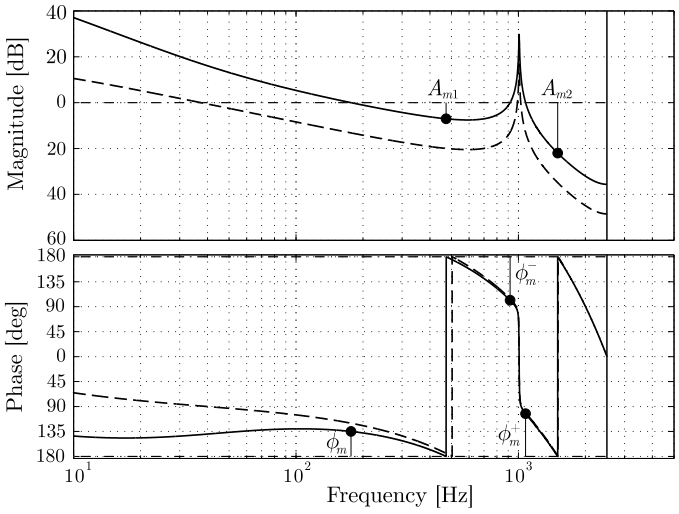

Fig. 6. Open-loop frequency response of (dotted) $P_2(z)$ and (dashed) $G_2(z)$ when damping is provided at the design stage changing ($f_s = 5$ kHz).

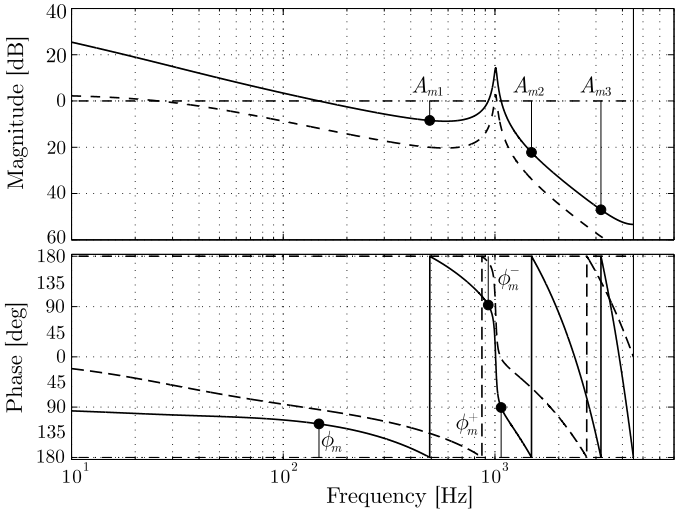

Fig. 7. Frequency response of (dotted) $P_2(z)$ ($f_s = 9$ kHz) and (solid) $G_2(z)$, when $D(z)$ is used to provide damping and $C_2(z)$ is PI controller with $\phi_m = 45$ deg.

D. Simulation Results

Fig. 8 shows the simulation results of a 25 A step change in i_{2-q}^*, for different current controllers. Fig. 8 (a) shows the results when $f_s = 5$ kHz. It can be seen that the transient is fast and that oscillations are well damped. Fig. 8 (b) shows the results for the same experiment, but in this case $f_s = 9$ kHz and $D(z)$ is not used. There are large oscillations in the grid

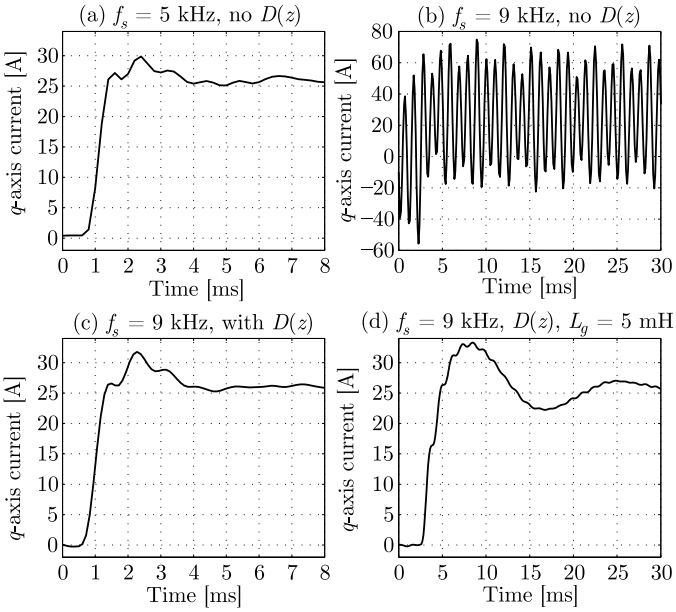

Fig. 8. Simulation results of the closed-loop system for (a) $f_s = 5$ kHz, $f_s = 9$ kHz (b) without and (c) with $D(z)$. (d) $f_s = 9$ kHz with $D(z)$ and $L_g = 5$ mH.

current and the system is very close to become unstable. Fig. 8 (c) shows the results when $f_s = 9$ kHz, but in this case $D(z)$ is applied. The transient is now well damped and the oscillation in Fig. 8 (b) has disappeared. It can be observed that the transient response is very similar to that in Fig. 8 (a). Finally, Fig. 8 (d) shows the transient response when $f_s = 9$ kHz, $D(z)$ is used, and $L_g = 5$ mH ($R_g = 0\ \Omega$). It can be seen that the transient response is slow, but the closed-loop system is still stable and that the high-frequency oscillation is well damped.

VII. Experimental Results

1) Active Damping Provided at the Design Stage: The sampling frequency is $f_s = 5$ kHz, so active damping is provided at the design stage as shown in Fig. 6 ($D(z)$ is not necessary). Fig. 9 (top) shows the transient performance of the VSC when the i^*_{2-q} is changed from 0 to 20 A (RMS). It can be seen that the transient response of the closed-loop system is perfectly damped and that there are no oscillations in the output current.

2) Active Damping Provided by the Controller: Fig. 10 shows the VSC output current when $D(z)$ is connected in series with the current controller. The sampling frequency is $f_s = 9$ kHz (see Fig. 7). It can be seen that the high-frequency oscillation disappears when $D(z)$ is connected. Fig. 9 (bottom) shows the transient performance of the VSC when the q-axis set-point is modified from 0 to 20 A (RMS). It can be seen that the transient response is slightly slower compared to the one in Fig. 9 (top), but sill fast.

VIII. Conclusion

This paper has shown a method to damp *LCL* filter resonances with a single control loop that is based on making

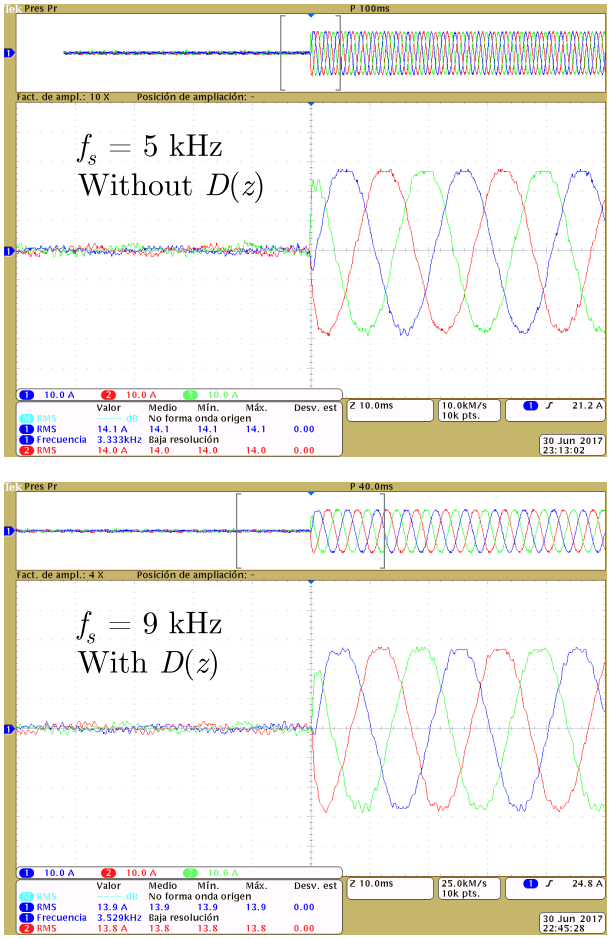

Fig. 9. Output current ($i_2(t)$) for a step-change in $i^*_{2-q}[k]$ when (top) $f_s = 5$ kHz and (bottom) $f_s = 9$ kHz with $D(z)$.

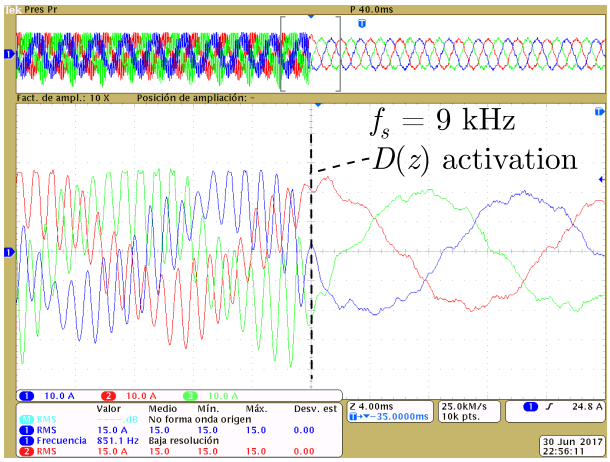

Fig. 10. Converter output current for $f_s = 9$ kHz when $D(z)$ is connected in series with the current controller.

zero the open-loop phase at the resonance frequency. It has been shown that this goal can be achieved at the design stage by changing a) the sampling period or b) the resonance frequency. However, when this is not possible, a solution based

on all-pass filters has been proposed. It has been shown that the simplest solution is to guarantee stability at the design stage: this simplifies the PI controller design and provides fast transient responses because no additional additional delay is added to the control loop. However, when this is not possible, a first-order all-pass filter is a simple solution. This solution is robust against changes in the grid impedance, but it slightly slows down the transient response. All the proposed control improvements have been verified by simulation and in a 15 kW prototype of a VSC connected to the grid with an *LCL* filter.

ACKNOWLEDGEMENTS

Thanks are due to Milan Prodanovic for his comments on this paper and to Norvento Energía Distribuida.

REFERENCES

[1] M. T. Bina and E. Pashajavid, "An efficient procedure to design passive LCL-filters for active power filters," *Electric Power Systems Research*, vol. 79, no. 4, pp. 606–614, 2009.

[2] R. Peña-Alzola, M. Liserre, F. Blaabjerg, R. Sebastián, J. Dannehl, and F. W. Fuchs, "Analysis of the passive damping losses in LCL-filter-based grid converters," *IEEE Transactions on Power Electronics*, vol. 28, no. 6, pp. 2642–2646, June 2013.

[3] R. N. Beres, X. Wang, F. Blaabjerg, M. Liserre, and C. L. Bak, "Optimal design of high-order passive-damped filters for grid-connected applications," *IEEE Transactions on Power Electronics*, vol. 31, no. 3, pp. 2083–2098, March 2016.

[4] R. Peña-Alzola, M. Liserre, F. Blaabjerg, R. Sebastián, J. Dannehl, and F. W. Fuchs, "Systematic design of the lead-lag network method for active damping in LCL-filter based three phase converters," *IEEE Transactions on Industrial Informatics*, vol. 10, no. 1, pp. 43–52, Feb 2014.

[5] C. A. Busada, S. G. Jorge, and J. A. Solsona, "Full-state feedback equivalent controller for active damping in LCL-filtered grid-connected inverters using a reduced number of sensors," *IEEE Transactions on Industrial Electronics*, vol. 62, no. 10, pp. 5993–6002, Oct 2015.

[6] T. N. Nguyen, A. Luo, and M. Li, "A simple and robust method for designing a multi-loop controller for three-phase VSI with an LCL-filter under uncertain system parameters," *Electric Power Systems Research*, vol. 117, pp. 94–103, 2014.

[7] J. Roldán-Pérez, A. García-Cerrada, J. L. Zamora-Macho, and M. Ochoa-Giménez, "Helping all generations of photo-voltaic inverters ride-through voltage sags," *IET Power Electronics*, vol. 7, no. 10, pp. 2555–2563, 2014.

[8] X. Wang, F. Blaabjerg, and P. C. Loh, "Virtual RC damping of LCL-filtered voltage source converters with extended selective harmonic compensation," *IEEE Transactions on Power Electronics*, vol. 30, no. 9, pp. 4726–4737, Sept 2015.

[9] X. Wang, C. Bao, X. Ruan, W. Li, and D. Pan, "Design considerations of digitally controlled LCL-filtered inverter with capacitor-current-feedback active damping," *IEEE Journal of Emerging and Selected Topics in Power Electronics*, vol. 2, no. 4, pp. 972–984, Dec 2014.

[10] B. C. Kuo and F. Golnaraghi, *Automatic Control Systems*, 8th ed. New York, NY, USA: John Wiley & Sons, Inc., 2002.

[11] F. Huerta, D. Pizarro, S. Cobreces, F. J. Rodriguez, C. Giron, and A. Rodriguez, "LQG servo controller for the current control of LCL grid-connected voltage-source converters," *IEEE Transactions on Industrial Electronics*, vol. 59, no. 11, pp. 4272–4284, Nov 2012.

[12] Y. A. R. I. Mohamed, M. A. Rahman, and R. Seethapathy, "Robust line-voltage sensorless control and synchronization of LCL-filtered distributed generation inverters for high power quality grid connection," *IEEE Trans. on Power Electronics*, vol. 27, no. 1, pp. 87–98, Jan 2012.

[13] X. Bao, F. Zhuo, Y. Tian, and P. Tan, "Simplified feedback linearization control of three-phase photovoltaic inverter with an LCL filter," *IEEE Trans. on Power Electronics*, vol. 28, no. 6, pp. 2739–2752, June 2013.

[14] W. Yao, Y. Yang, X. Zhang, F. Blaabjerg, and P. C. Loh, "Design and analysis of robust active damping for LCL filters using digital notch filters," *IEEE Transactions on Power Electronics*, vol. 32, no. 3, pp. 2360–2375, March 2017.

[15] X. Fu and S. Li, "Control of single-phase grid-connected converters with LCL filters using recurrent neural network and conventional control methods," *IEEE Transactions on Power Electronics*, vol. 31, no. 7, pp. 5354–5364, July 2016.

[16] H. Komurcugil, S. Ozdemir, I. Sefa, N. Altin, and O. Kukrer, "Sliding-mode control for single-phase grid-connected LCL-filtered VSI with double-band hysteresis scheme," *IEEE Transactions on Industrial Electronics*, vol. 63, no. 2, pp. 864–873, Feb 2016.

[17] Y. Lyu, H. Lin, and Y. Cui, "Stability analysis of digitally controlled LCL-type grid-connected inverter considering the delay effect," *IET Power Electronics*, vol. 8, no. 9, pp. 1651–1660, 2015.

[18] J. Wang, J. D. Yan, L. Jiang, and J. Zou, "Delay-dependent stability of single-loop controlled grid-connected inverters with LCL filters," *IEEE Trans. on Power Electronics*, vol. 31, no. 1, pp. 743–757, Jan 2016.

[19] C. Chen, J. Xiong, Z. Wan, J. Lei, and K. Zhang, "A time delay compensation method based on area equivalence for active damping of an LCL-type converter," *IEEE Transactions on Power Electronics*, vol. 32, no. 1, pp. 762–772, Jan 2017.

[20] A. Yazdani and R. Iravani, *Voltage-Sourced Converters in Power Systems*. Wiley, 2010.

[21] B. Kuo, *Digital Control Systems*. Oxford University Press, 1992.

[22] J. Roldán-Pérez, A. García-Cerrada, J. L. Zamora-Macho, P. Roncero-Sánchez, and E. Acha, "Troubleshooting a digital repetitive controller for a versatile dynamic voltage restorer," *International Journal of Electrical Power & Energy Systems*, vol. 57, no. 0, pp. 105–115, 2014.

[23] T. Laakso, V. Valimaki, M. Karjalainen, and U. Laine, "Splitting the unit delay [FIR/all pass filters design]," *IEEE Signal Processing Magazine*, vol. 13, no. 1, pp. 30–60, 1996.

[24] M. Alakula and A. Carlsson, "An induction machine servo with one current controller and an improved flux observer," in *Industrial Electronics, Control, and Instrumentation, 1993. Proceedings of the IECON '93., International Conference on*, Nov 1993, pp. 1991–1996 vol.3.